9-1-2002

Investigation of Lower-limb Tissue Perfusion during Loading

Barbara Silver-Thorn
Marquette University, barbara.silver-thorn@marquette.edu

Published version. *Journal of Rehabilitation Research and Development*, Vol. 39, No. 5 (September/October 2002): 597-608. Permalink.

Department of Veterans Affairs

Journal of Rehabilitation Research and Development
Vol. 39 No. 5, September/October 2002
Pages 597–608

Investigation of lower-limb tissue perfusion during loading

M.B. Silver-Thorn, PhD
Marquette University, Department of Biomedical Engineering, 1515 West Wisconsin Avenue, Olin Engineering Center, Room 338A, Milwaukee, WI

Abstract—An extant tissue indentor used for amputee residual limb tissue indentation studies was modified to include laser Doppler flowmetry (LDF) to enable measurement of tissue perfusion during indentation. This device allows quantitative assessment of the mechanical and physiological response of soft tissues to load, as demonstrated by indentation studies of the lower-limb tissues of young healthy subjects. Potential measures of interest include the relative change in tissue perfusion with load and the time delays associated with the perfusion response during tissue loading and unloading. Such measures may prove useful in future studies of residual limb tissues, improving our understanding of tissue viability risk factors for individuals with lower-limb amputation.

Key words: *blood flow, indentation, perfusion, tissue.*

INTRODUCTION

Today, the United States has approximately 400,000 amputees. Of these amputations, 90 percent involve the lower limb (55 percent transtibial, 30 percent transfemoral, and 5 percent partial foot). The majority (75 percent) of these amputations result from disease, most commonly peripheral vascular disease [1].

Address all correspondence and requests for reprints to M.B. Silver-Thorn, PhD; Marquette University, Department of Biomedical Engineering, 1515 West Wisconsin Avenue, Olin Engineering Center, Room 338A, Milwaukee, WI 53233; 414-288-3608; fax: 414-288-7938; email: B.Silver-Thorn@Marquette.edu.

Many of the prostheses fabricated for these amputees are not satisfactory. Poor fit results in discomfort and pain for the amputee and may impair amputee mobility and/or contribute to tissue degradation. This tissue degradation is particularly serious for vascular amputees, because their ability to heal is often impaired.

Investigators have looked at stress, specifically the interface stress between the residual limb and prosthetic socket, as a potential objective measure of prosthetic fit. However, this parameter is difficult to reliably measure [2–4], and computer models of the residual limb have not yet yielded accurate estimates of the interface stress [2,5,6]. Because tissue ischemia caused by inadequate perfusion is believed to be a primary cause of pressure sore development [7–12], tissue perfusion measures may provide a means of advancing our definition of prosthetic fit.

Vascular Measures Related to Amputation and Wound Healing

Because more proximal levels of lower-limb amputation increase energy costs for ambulation [13,14], surgeons select the most distal level of amputation likely to heal. Clinical criteria such as pulse status, limb color, temperature, infection, necrosis, and wound bleeding have been inconsistent predictors of amputation healing [15]. Numerous noninvasive (thermography, transcutaneous oximetry [tcpO_2], laser Doppler flowmetry [LDF], photoplethysmography, Doppler ankle-brachial indices) and invasive (^{133}Xe skin clearance, fluorescein dye angiography) measures have been investigated as potential objective criteria for selection of the amputation level [16–23]. Similar studies have been performed to evaluate

and/or predict wound healing and the treatment of ischemic ulcers [24,25]. While each measure has some utility, none has demonstrated sufficient sensitivity and specificity to warrant universal adoption.

While LDF may not provide definitive information regarding the likelihood of wound healing, it does provide information regarding local tissue perfusion. This measure is noninvasive, quick to estimate, and readily applied to multiple sites or areas of the body. In principle, LDF measures blood flux in the microvasculature, the capillaries close to the skin surface, and the underlying arterioles and venules involved in the regulation of skin temperature. Low-power light from a monochromatic laser, incident on tissue, is scattered by moving red blood cells and undergoes a change in wavelength. This "Doppler shift" is converted to "perfusion" units, related to the product of mean cell velocity and average concentration of moving blood cells by commercial LDF systems. The LDF measurement depth depends on the underlying physiology, incident light, and fiber separation between transmitting and receiving fibers and is typically less than 1 mm.

Applications of LDF often involve investigation of perfusion in response to provocation, such as application of heat or vessel occlusion. The relative change in tissue perfusion, as well as the initial rate of change and time to equilibrate, in response to this provocation has potential diagnostic value in assessing vascular function. Schubert and Fagrell [26,27] used LDF to measure skin blood cell flux and temperature to investigate the human microvascular response to external pressure to assess risk of decubitus ulcer formation. The LDF measures confirmed the existence of microvascular differences between the sacral and gluteal tissues contributing to increased frequency of ulceration at the sacrum. A similar animal study by Salcido et al. [28] attempted to quantify the critical threshold of reduced blood flow because of external pressure leading to pressure sore formation. Their system included an electromechanical pressure delivery system for generating experimentally derived pressure ulcers while monitoring blood perfusion using LDF. Similarly, Zhang and Roberts [29] used skin blood flow as measured by LDF to investigate the effects of shear forces applied to human tissues.

Mechanical and Physiologic Effects of Soft Tissue Loading

Human soft tissues consist of a variety of macrostructures, including skin, skeletal muscle, artery, vein, cartilage, ligament, and tendon. Soft tissue studies have typically focused on isolated structures by using in vitro experiments to quantify the mechanical loading response and to formulate constitutive equations.

Numerical models of the residual limb require in vivo description of bulk amputee soft tissues in compression. Such in vivo investigations typically involve indentor studies [30–37]. These studies indicate that the response of human bulk soft tissue to compressive load is nonlinear, is time-dependent, exhibits stress-relaxation, and varies as a function of the loading rate and level of muscle activation.

While quantifying the mechanical response of human tissues to load is important, understanding the corresponding physiological response to load is vital. Such knowledge would help prevent pressures sores and perhaps provide insight into tissue remodeling so that tissues that are routinely exposed to load (i.e., plantar tissues, buttocks tissues for spinal cord injured persons, residual-limb tissues for lower-limb amputees) might be "conditioned."

Mechanical and physiological analysis of soft tissues has attempted to define load-duration thresholds using animal models [7,28,38–41]. The influence of shear forces and friction on these thresholds has also been investigated [9,38,42]. While there has not been a consensus regarding absolute thresholds, an inverse load-duration relationship has been acknowledged. Pressure-induced ischemia is believed to be a primary factor influencing decubitus ulcer formation [43].

The purpose of this study was to augment a device used previously to assess the in vivo nonlinear, viscoelastic mechanical response of human soft tissue to load, to include measures of tissue perfusion. Preliminary indentation studies that used the modified device were conducted to demonstrate the utility of such a tool and to identify potential measures of interest.

METHODOLOGY

Original Tissue Indentor System

An extant rate-controlled indentor [44,45] that was used to characterize the force-displacement behavior, force-relaxation, and creep response of residual-limb soft tissues was modified to investigate tissue perfusion. Rate-controlled indentation was implemented with a linear actuator; the indentor also incorporated a compression load cell so the reaction force to indentation could be

measured.* The linear actuator and data acquisition were controlled via two digital I/O (input/output) cards for the PCMCIA [peripheral component microchannel interconnect architecture (IBM)] bus of a laptop personal computer and LabVIEW for Windows.†

Hardware Modifications

Simultaneous measurement of tissue perfusion was enabled by the extant indentor being interfaced with a commercial laser Doppler perfusion measurement system.‡ An endoscopic probe was custom designed so that the fiber separation between the transmitting and receiving optical fibers was maximized to 500 μm (default fiber separation was 250 μm);§ the external diameter remained at 1.9 mm. The increased fiber separation maximized the measurement depth and yet ensured the fiber could still be housed within the 4 mm indentor tip. The flexibility of this probe facilitated threading the probe into the indentor tip.

The original indentor shaft-tip was removed from the indentor. The solid single piece design was modified to form two distinct pieces so that the concentric perfusion probe was secured as the two pieces were screwed together (**Figure 1**). The smaller diameter tip was bored to accommodate the perfusion probe; it was tapered, externally threaded, and slotted at one end to secure it to the larger diameter indentor shaft. This shaft had a hole bored through the center and out one side at a wide angle to form a channel for the perfusion probe. The shaft was internally threaded at one end to attach to the load cell; the other end was internally threaded to accommodate the indentor tip.

After the modified indentor shaft was secured onto the load cell, the perfusion probe was fed through the access slot into the channel of the shaft. It was similarly fed through the indentor tip, external to the indentor. The tip was then threaded onto the shaft, such that the perfusion probe and indentor tip were flush. The perfusion probe was secured as the tapered end of the indentor tip was threaded onto the indentor shaft. The probe cable was then connected to the PeriFlux 5000 front panel.

Next, the analog output on the rear of the PeriFlux 5000 was connected (via an RS-232-banana-plug cable) to the analog-to-digital terminal blocks contained in the signal conditioning box of the indentor system. This facilitated simultaneous acquisition of perfusion and force during indentation. Conversion of the perfusion signals to arbitrary perfusion units (apu) was performed with the use of a motility standard.¶

Software Modifications

The LabVIEW virtual instruments (VIs) controlling the indentor motor and data acquisition were modified to include sampling of tissue perfusion. The PeriFlux 5000 system includes hardware filters with cutoff frequencies (–3 dB point) of 0.125, 1.25, and 7.5 Hz.** For this preliminary testing, the hardware filter was 7.5 Hz, unless otherwise noted. The two PeriFlux analog outputs, perfusion and the total amount of returning light or total backscatter, were sampled at 100 Hz (40 Hz for creep testing). The indentor force was sampled at 300 Hz for cyclic loading and relaxation trials and at 40 Hz for creep trials. The perfusion data were then plotted, along with the force and displacement data, and were appended to the corresponding output files.

Test Protocol

The original device enabled in vivo testing of the lower-limb soft tissues [46,47]. Testing included rate-controlled cyclic loading, force relaxation, and creep protocols. These protocols were also used for the preliminary tissue loading-perfusion studies.

*The line actuator was model L92421-P1 (0.05 mm per pulse) with model K33505 drive card, Philips Airpax Ltd., Cheshire, Connecticut. The load cell was model 31/1426-04-03 (0 to 44 N), Sensotec, Columbus, Ohio.

†The I/O card was the Multifunction DAQCard-1200, National Instruments, Austin, Texas. LabVIEW version 5.0 was used, National Instruments, Austin, Texas.

‡PeriFlux (PF) System 5000 (PF 5001 main unit; PF 5010 laser Doppler unit), Perimed AB, Stockholm, Sweden.

§Model 409 endoscopic probe, Perimed AB, Stockholm, Sweden.

¶The motility standard, PF1001, is a colloidal suspension of latex particles. Brownian motion of these latex particles provides a standardized perfusion value equivalent to 250 perfusion units (pu) (250 ± 5% at 22 °C). One perfusion unit corresponds to 10 mV. Zeroing is automatic. The perfusion unit is arbitrary and cannot be given any physiological definition such as actual number of cells flowing through a given volume of tissue during a given time period. Thus, the perfusion units are not absolute. As such, they are referred to as arbitrary perfusion units (apu).

**These low-pass filters correspond to time constants of 3.0, 0.2, and 0.03 s, respectively, on the PeriFlux 5000 front panel.

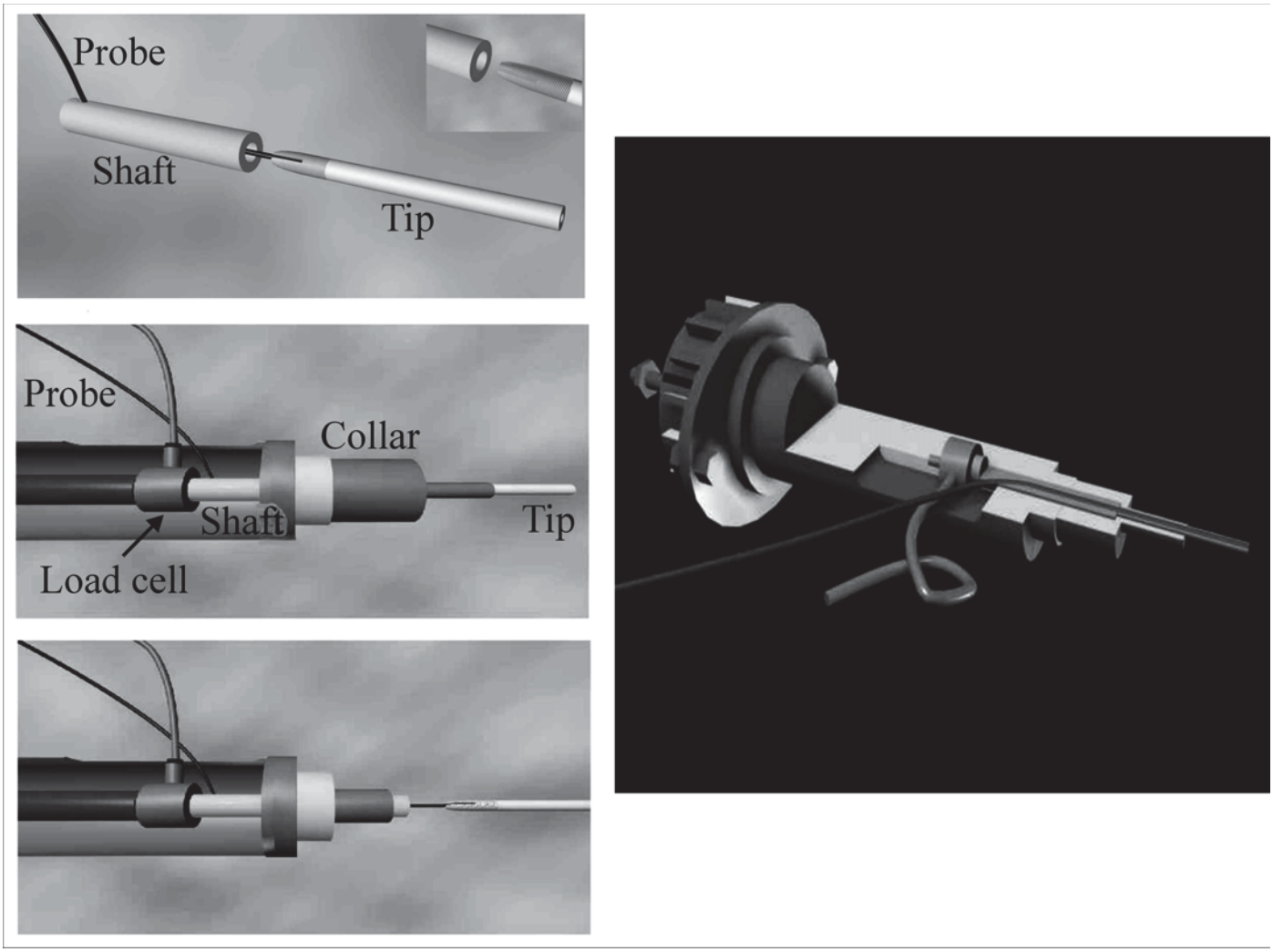

Figure 1.
Modified two-piece indentor shaft-tip that accommodates and secures perfusion probe.

Institution Review Board (IRB) approval was obtained for the modified indentor-perfusion system and associated test protocols. Subject selection criteria were young (less than 40 years), healthy subjects with no prior history of dermatological or vascular problems. In vivo indentation tests of the soft tissues of the right calf for 19 individuals (see **Table**) were conducted. As tissue perfusion is temperature and "stress" dependent, each subject acclimated to the room and his or her surroundings for 15 minutes before testing began.

Following informed consent, a "pseudosocket" consisting of a test port-Velcro strap was positioned over the posterior calf (**Figure 2**). This pseudosocket facilitated mounting the tissue indentor so that indentation was perpendicular to the limb surface. Before the indentor studies were initiated, the maximum tissue indentation that could be tolerated without discomfort (d_{max}) was manually evaluated with an indentor-like probe. All subsequent indentor trials were conducted with indentations less than 85% d_{max}.

The LDF probe was calibrated with the use of the motility standard (see note on previous page) before subject testing. Because calibration requires that the indentor tip be removed from the load cell and the LDF probe removed from the tip, calibration preceded testing of the first subject. However, ambient light noise (as indicated by the variable total backscatter during testing of Subject 6)

Table.
Summary of test subjects.

Subject	Age (yr)	Gender	Calibrated Probe
1	20	F	Y
2	23	F	N*
3	26	M	N
4	27	M	N
5	22	M	N
6	24	M	N
7	22	F	Y
8	27	M	Y
9	34	M	Y
10	23	M	Y
11	37	F	Y
12	34	M	Y
13	37	F	Y
14	22	F	Y
15	22	F	Y
16	24	M	Y
17	24	M	Y
18	24	F	Y*
19	20	F	Y

Y = yes
N = no
*Perfusion hardware filter cutoff frequency was 1.25 Hz, as opposed to default cutoff frequency used for all other subjects was 7.5 Hz.

indicated that such calibration should be conducted before each subject was tested.*

Force-perfusion data were collected during 10 loading and unloading cycles at indentation rates of 1, 5, and 10 mm/s (randomly selected). An additional test for the assessment of force-relaxation and the associated tissue perfusion was also conducted. During this relaxation test, the respective tissues were indented at 5 mm/s to a prescribed displacement (less than 85% d_{max}). The tissue force and perfusion were then monitored, with no additional indentation, for 30 s. While relaxation trials conducted with the original indentor were 120 s, the acquisition of the additional perfusion (and total backscatter) data resulted in file size limitations (i.e., buffer overflows), necessitating the reduced test duration. Finally, tissue studies for the evaluation of creep and the associated tissue perfusion were conducted. During these creep tests, the tissues were indented at 1 mm/s. The tissue creep and perfusion were then monitored while the tissue was

*Perimed AB recommends calibration only when the probes are changed.

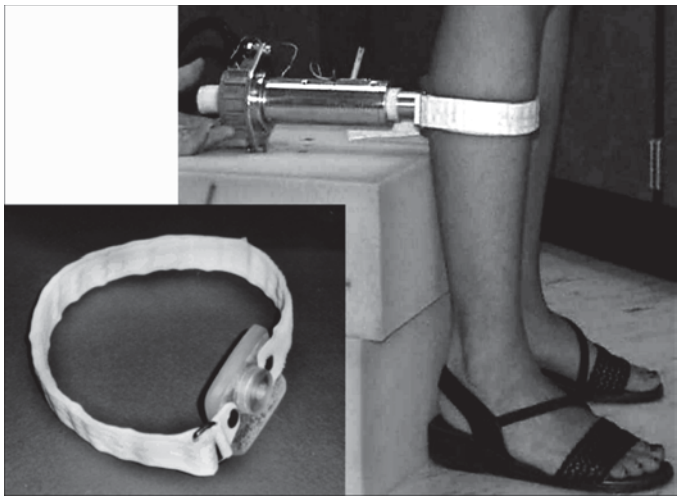

Figure 2.
Pseudosocket (left) used to position indentor over the tissues of posterior calf.

subjected to a constant force (less than the peak force observed during the initial 1 mm/s cyclic loading) for 100 s. As for the relaxation trials, the original creep test duration (120 s) was reduced to accommodate the additional data channels.

Signal Processing

Prior to signal processing specific to the respective test protocols, the force and perfusion data were digitally low pass filtered at 5 Hz (LabVIEW®).†

Cyclic Loading Data

Force-time and perfusion-time curves were obtained for rate-controlled cyclic loading (**Figure 3(a)** and **3(b)**). Contact of the indentor tip with the limb surface was defined by the force amplitude, namely, when the force exceeded the "no-load" force by 0.2 N. The data cycles were subdivided into the respective loading and unloading portions, based on this contact force (start of tissue loading, end of tissue unloading) and the maximum force of the respective cycle (end of tissue loading, beginning of tissue unloading), as shown in **Figure 3(b)**.

Analysis of the loading data were conducted to determine the loading delay, defined as the time between the onset of tissue loading and the subsequent decrease in tissue perfusion. Two different techniques were used to estimate this

†For cyclic and relaxation data, this filter was implemented with the use of a 7.8 Hz second-order Butterworth filter and applied forward and backward, thereby minimizing phase lag. For creep, a 5 Hz fifth-order elliptical filter was used.

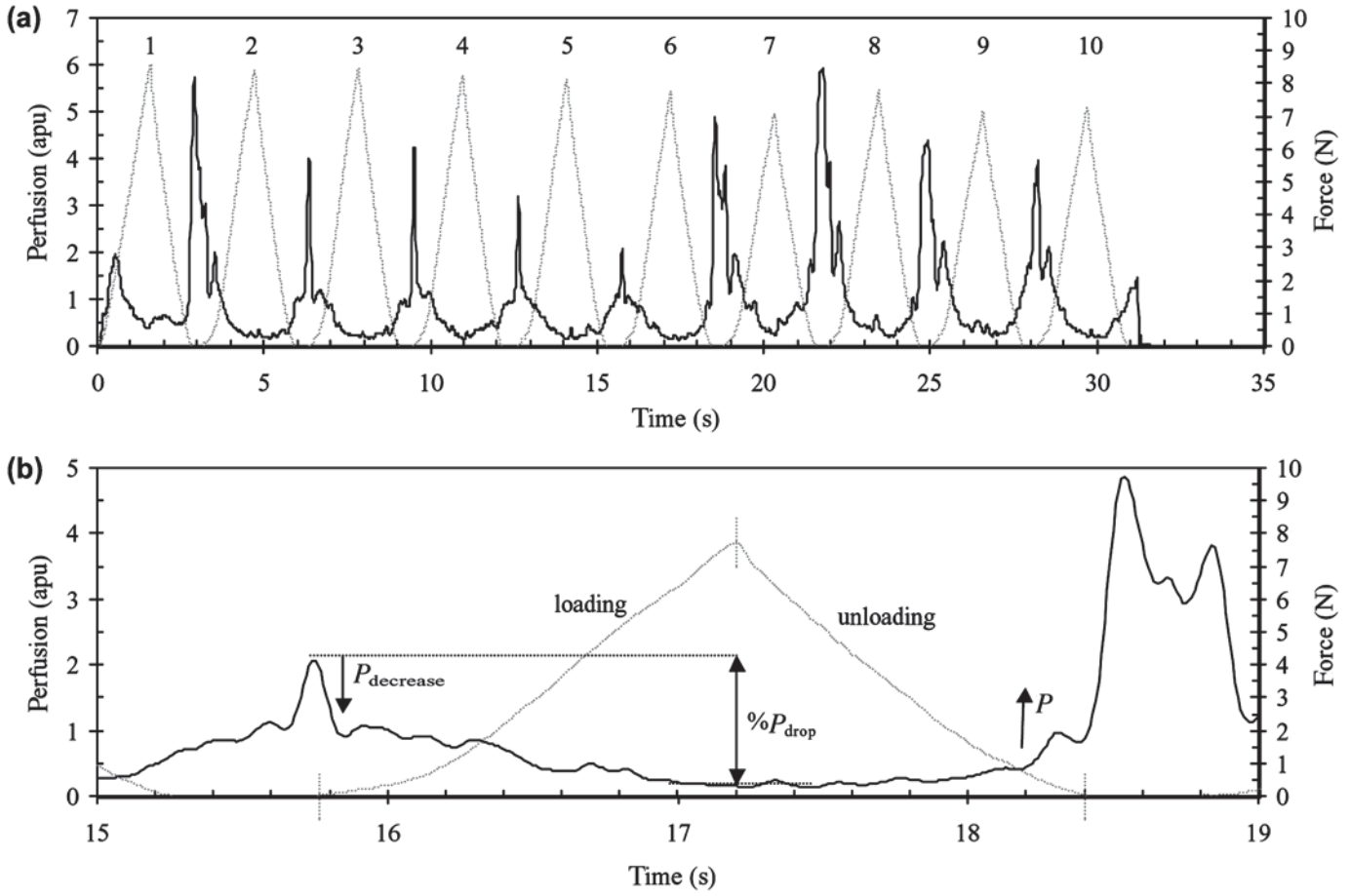

Figure 3.
Representative data for cyclic loading for Subject 16 at 5 mm/s (force = gray; perfusion = black). Shown are **(a)** all 10 loading and unloading cycles and **(b)** a close-up of cycle 6.

parameter, one based on a threshold detection scheme and the second based on the maximum cross-correlation coefficient.

For the threshold detection scheme, the change in perfusion was approximated by central difference techniques

$$\text{at time, } t = t_n, \qquad \frac{dP}{dt} = \frac{(P_{n+1} - P_{n-1})}{2\Delta t} \ ,$$

where P is the tissue perfusion (apu), t is time (s), n is the sample number, and $\Delta t (= 1/f_S = 1/100 \text{ Hz})$ is 10 ms. The onset of tissue perfusion decrease was determined based on a perfusion slope threshold detection scheme so that the time of perfusion decrease, $t_{P\text{decrease}}$, occurred when

$$|dP/dt| > dP/dp_{\text{threshold}} (\text{where } dP/dt < 0) \ .$$

The loading delay was also estimated with the Hilbert transform. The resultant maximum cross-correlation coefficient provides an estimate of the delay between the force and perfusion time series for each of the respective 10 loading time series. These delays were then averaged for all cycles at the respective indentation rate. More specific details regarding the use of this methodology are reviewed by Saad et al. [48].

The associated magnitude of the physiologic or perfusion response, $\%P_{\text{drop}}$, was defined as the normalized change in maximum (P_{max}) and minimum (P_{min}) tissue perfusion for each cycle

$$\%P_{\text{drop}} = \frac{(P_{\text{max}} - P_{\text{min}})}{P_{\text{max}}} * 100 \ .$$

This physiologic response was then averaged over the respective 10 cycles at each indentation rate.

The mean recovery delay was similarly evaluated based on the unloading data, defined as the time between the onset of tissue unloading and the subsequent increase in tissue perfusion.

Relaxation Data

Force-time and perfusion-time curves were also obtained for the relaxation (ramped step displacement) loading. Contact of the indentor tip with the limb surface was again defined by the force amplitude. The data were divided into the respective initial loading and relaxation portions, based on the contact force (start of tissue loading) and the maximum force (end of tissue loading, beginning of the relaxation period), as shown in **Figure 4**.

The associated magnitude of the physiologic or perfusion response ($\%P_{drop}$) was evaluated as for cyclic loading. The mechanical response was quantified in terms of the percentage of force relaxation, $\%f_{rlxn}$,

$$\%f_{rlxn} = \frac{(f_{max} - f_{equilibrium})}{f_{max}} * 100 \ ,$$

where $f_{equilibrium}$ was the mean force over the final 2 s of relaxation. The equilibrated or steady state perfusion, $P_{equilibrium}$, was similarly evaluated. Finally, the time for the tissue to equilibrate, $t_{equilibrium}$, defined as the time for the tissue to fall to this $P_{equilibrium}$ value, was evaluated.

Creep Data

Force-time, displacement-time, and perfusion-time curves were obtained for the creep (constant force) loading. Contact of the indentor tip with the limb surface was again defined by the force amplitude. The data were divided into the respective initial loading and creep portions, based on this contact force (start of tissue loading) and the time at which the force reached its target value (end of tissue loading, beginning of creep period), as shown in **Figure 5**.

The associated magnitude of the physiologic or perfusion response ($\%P_{drop}$) was evaluated as described previously. The mechanical response was quantified in terms of the percentage of tissue creep,

$$\%\text{creep} = \frac{(d_{equilibrium} - d_{f\,target})}{d_{f\,target}} * 100 \ ,$$

where $d_{f\,target}$ is the initial displacement when the force reached the target load and $d_{equilibrium}$ is the mean displacement over the final 15 s of loading. The equilibrated or steady state perfusion was also evaluated over the final 15 s of loading. Finally, the time for the tissue to equilibrate, $t_{equilibrium}$, defined as the time for the tissue to fall to within 95 percent of $P_{equilibrium}$, was also evaluated.

RESULTS

Preliminary tests conducted with the modified device did not indicate any degradation in initial system performance. Frequency analysis of the perfusion (and total backscatter) data indicated that the signal power was consistently less than 5 Hz for all test protocols for the first six subjects tested. In subsequent studies, the 100 Hz sampling rate for perfusion (and total backscatter) can be reduced to enable longer test duration and indentations.

The total backscatter measure depends on the power, alignment, and focusing of the laser, as well as the light scattered by the blood cells. Since hemoglobin in red blood cells absorbs light, the higher the blood cell concentration, the less the light reflected and hence the lower the total backscatter value. The total backscatter is therefore correlated to the blood cell content of tissue rather than blood flow. Total backscatter can also be considered as a measure of the total amount of light returned. As such, it is a means with which to identify experimental error. Perimed AB recommends that the total backscatter measure during testing be [0.5, 9.5 V]. If the total backscatter is outside this range, the accompanying perfusion data are considered suspect. The perfusion probe should then be recalibrated. During testing of the calf tissues of the 19 subjects for each of the five test protocols, the total backscatter exceeded the recommended values for only one subject (Subject 6). Calibration of the perfusion probe was conducted before testing for all subjects after this error was noted.

Representative data for cyclic loading are illustrated in **Figure 3**. The overall mechanical (maximum force, f_{max}) and physiologic ($\%P_{drop}$) response as a function of indentation rate is summarized in **Figure 6**. The observed differences in physiologic response at the various indentation rates were statistically significant ($P < 0.005$ for 1 versus 5 mm/s; $P < 0.001$ for 5 versus 10 mm/s and 1 versus 10 mm/s).

The loading delay as estimated by the threshold detection scheme was dependent on the value of the slope threshold (**Figure 7a**). The alternative loading delay estimation scheme based on the maximum cross-correlation coefficient and the Hilbert transform appeared to be more robust, facilitating estimation of both the loading and unloading (recovery) delays for all cycles for all subjects (**Figure 7b**). The differences in the loading delays at the various indentation rates were also statistically significant ($P < 0.1$ for 1 versus 5 mm/s; $P < 0.005$ for 5 versus 10 mm/s; $P < 0.001$ for 1 versus 10 mm/s). The recovery

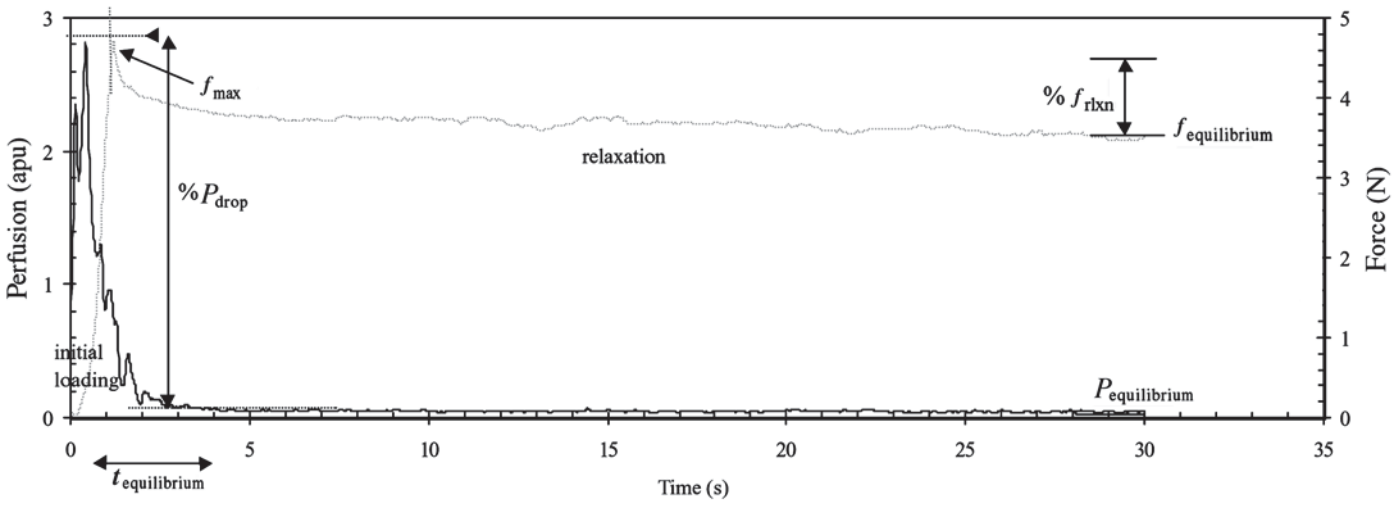

Figure 4.
Representative force (gray) and perfusion (black) data for relaxation (ramped step displacement) for Subject 9.

delays evaluated for the 19 subjects at each of the three indentation rates (as summarized in **Figure 7b)** were also found to differ significantly with the indentation rate ($P < 0.1$ for 1 versus 5 mm/s; $P < 0.005$ for 5 versus 10 mm/s; $P < 0.025$ for 1 versus 10 mm/s).

Representative data for relaxation loading are illustrated in **Figure 4.** As seen in this curve, little to no tissue reperfusion was observed during the relaxation period. The magnitude of the mechanical (f_{max}, $\%f_{rlxn}$) and physiologic ($\%P_{drop}$, $t_{equilibrium}$) response to the applied displacement is shown in **Figure 8**.

Finally, representative data for creep loading are illustrated in **Figure 5**. As seen in this curve, perfusion (black) does not continue to decrease as the tissue creeps. For the tissues tested to date, the applied force of 3.4 ± 1.2 N was accompanied by substantial tissue creep (313.4 ± 60.6%). The corresponding decrease in tissue perfusion was 89.3 ± 7.4%, with the perfusion falling to 95 percent of the equilibrated value in 1.35 ± 2.2 s.

DISCUSSION

The objectives of this work were to develop a tool to investigate tissue perfusion during loading, to demonstrate the utility of this device, and to identify potential perfusion measures of interest for future investigation of residual limb tissues.

The modified extant indentor retained the original functional capabilities and facilitated simultaneous measurement of tissue perfusion during cyclic loading, relaxation (ramped step displacement), and creep (constant force) loading. Limitations regarding the data acquisition card buffer (64 kB) were noted, necessitating reduced test duration for relaxation and creep loading—in addition to a maximum of 8 mm indentation at 1 mm/s. However, the observed frequency content of the perfusion data (less than 5 Hz) indicates that the 100 Hz sampling rate (40 Hz for creep loading) can be reduced substantially during future testing, obviating this hardware limitation.

The preliminary tissue loading-perfusion studies conducted on the posterior calf on young healthy subjects demonstrated the feasibility of such simultaneous measurements and the potential utility of the device. These preliminary studies identified the need for calibration of the perfusion probe before each subject was tested (as indicated by total backscatter outside the recommended [0.5, 9.5 V] range). While the cyclic, relaxation, and creep protocols were supported, the perfusion data during cyclic loading at 1 mm/s was noisier and less consistent from cycle to cycle than that observed at 5 and 10 mm/s. Future cyclic loading studies are therefore recommended at 5 and 10 mm/s only.

These preliminary indentation studies also identified potential perfusion measures of interest that might elucidate prosthetic fit and dermatological damage risk factors in lower-limb amputees and individuals with peripheral vascular disease. These measures of interest include the loading-recovery delays during cyclic loading; the time for the tissue perfusion to equilibrate during relaxation

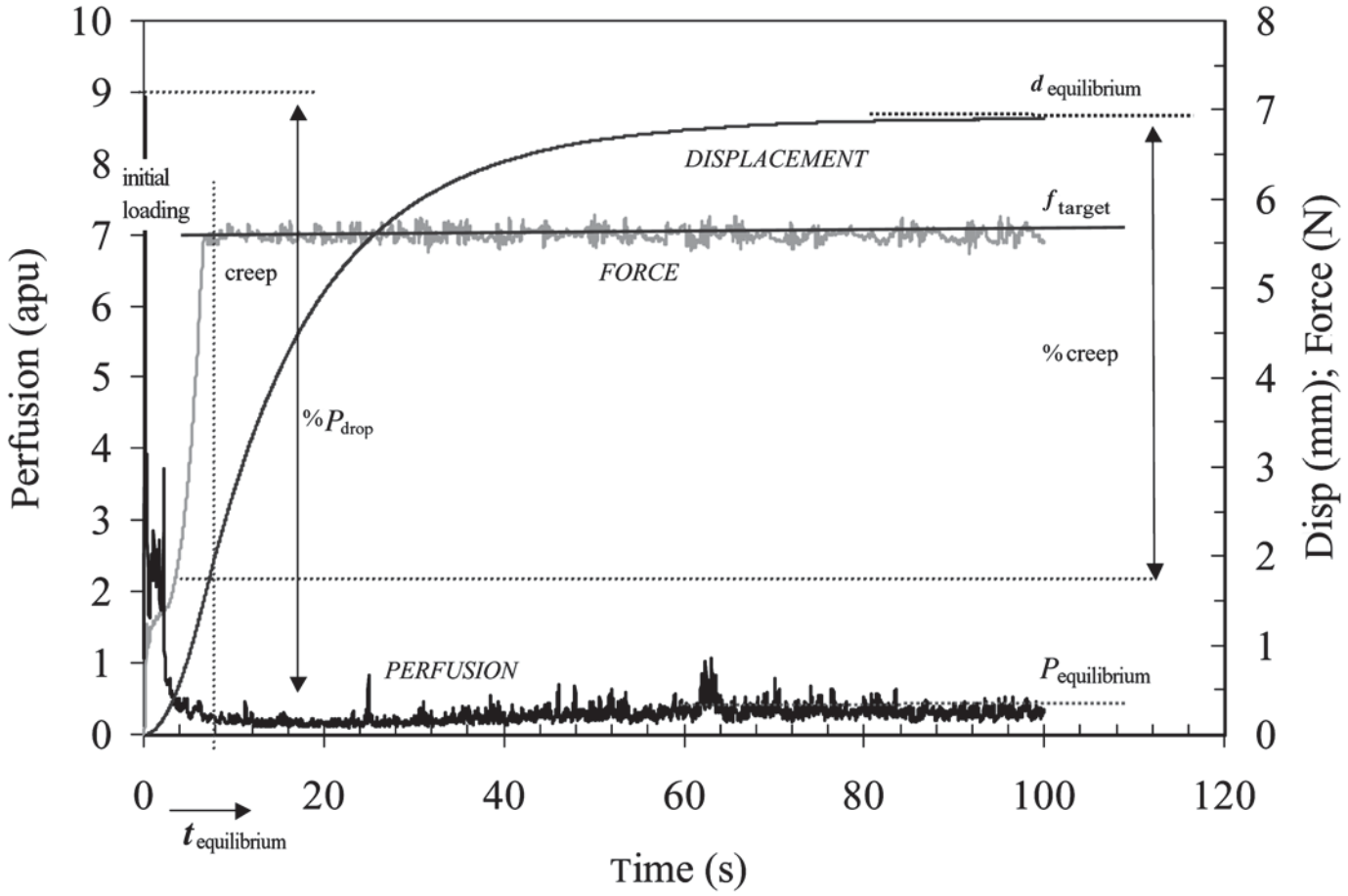

Figure 5.
Representative perfusion (black) and tissue creep (gray) in response to constant force (light gray) for Subject 17. Also shown are mechanical (f_{target} = 5.6 N, $d_{equilibrium}$ = 6.9 mm, $\%_{creep}$ = 331%) and physiologic ($\%P_{drop}$ = 95%, $P_{equilibrium}$ = 0.4 apu, $t_{equilibrium}$ = 3.1 s) measures of interest.

and creep loading; and the magnitude of the perfusion response during cyclic, relaxation, and creep loading.

The loading-recovery delays associated with cyclic loading were readily estimated with the cross-correlation coefficient and the Hilbert transform. More simplistic attempts based upon a perfusion slope threshold detection scheme were less robust and depended on the magnitude of the slope threshold. The estimated loading-recovery delays typically ranged from 1 s to 5 s, and varied with indentation rate (delays decreased as indentation rate increased). Statistical comparison (paired t-test) of the loading versus recovery delays indicated that the loading delay exceeded the recovery delay at 5 mm/s and 10 mm/s ($P < 0.001$ and $P < 0.05$, respectively). The difference in loading versus recovery delays at 1 mm/s was not significant, providing further incentive for the potential omission of this protocol in future studies.

The perfusion response, $\%P_{drop}$, during cyclic loading was substantial, ranging from 60 to 90 percent for *submaximal* loading of these tissues. This decrease in tissue perfusion was rate-dependent, with greater decreases observed at slower loading rates.

The physiologic explanation of these rate-dependent responses in the loading-recovery delays and perfusion decrease is not known. Further investigation is warranted to confirm the existence of such trends in larger populations and to determine if such behavior is also observed for limb tissues of individuals with vascular disease and/or lower-limb amputation.

The decreased force and perfusion during relaxation (ramped step displacement) testing was also marked, as

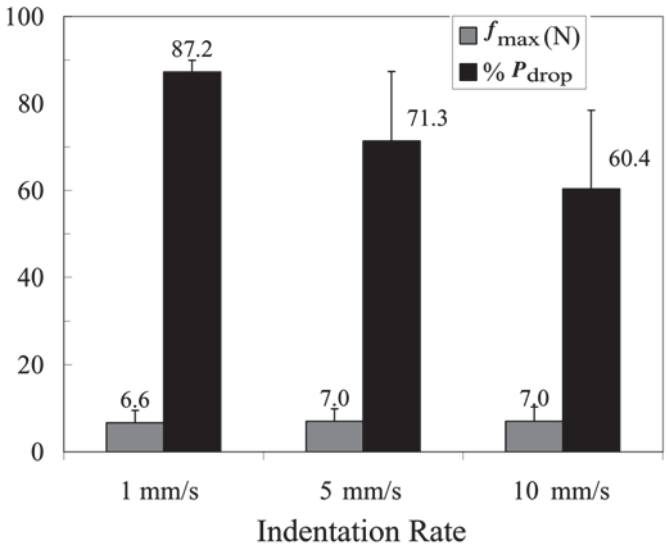

Figure 6.
Mechanical (maximum force, f_{max} [gray]) and physiologic (perfusion, $\%P_{drop}$ [black]) response to cyclic loading as a function of indentation rate.

seen in **Figure 8**. Perfusion in these posterior calf tissues typically equilibrated within 7 s to 9 s. While a reduced perfusion-sampling rate would permit relaxation duration greater than 30 s, this test period was sufficient to observe equilibrium. Future studies incorporating longer test periods may therefore not be necessary, although other sites and sample populations may exhibit different behavior.

Substantial tissue creep (more than 300 percent) and perfusion decreases (90 percent) were observed during constant force loading. The tissue perfusion typically equilibrated in 1 s to 4 s. As such, the 100 s test duration during creep testing was more than sufficient. Further investigation of lower-limb tissues for individuals with vascular disease and/or lower-limb amputation is warranted for one to determine whether the perfusion decrease and/or equilibrium time during creep (and relaxation) loading differs for these populations.

As tissue perfusion is temperature-dependent, future studies should also monitor ambient and skin temperature. Changes in tissue perfusion because of thermal variations may then be isolated.

CONCLUSION

This study resulted in a tool and some preliminary data with which to assess tissue perfusion as a function of load. The results of this preliminary work indicate that such studies are possible and that perfusion parameters such as the loading-recovery delay, equilibrium time, and perfusion decrease may have clinical utility. Future studies involving individuals with peripheral vascular disease and/or lower-limb amputation are needed.

ACKNOWLEDGMENTS

I thank M. Erkert, S. Lamont, T. Le, R. Shaw, and L. Treiber for their assistance with the mechanical coupling

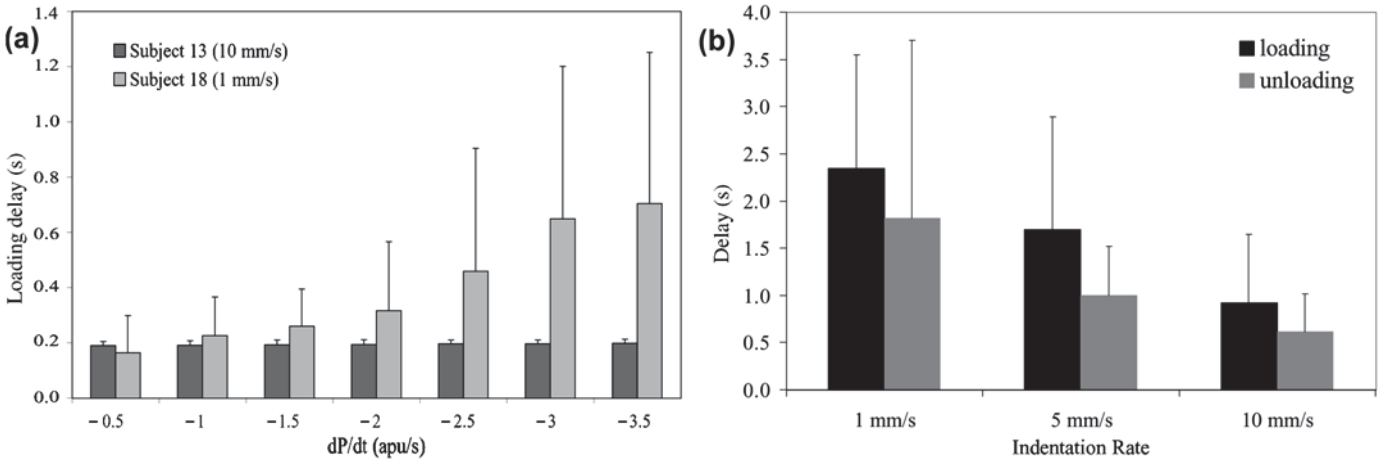

Figure 7.
(a) Dependence of mean loading delay on perfusion slope threshold for 10 loading cycles for Subjects 13 (10 mm/s, black) and 18 (1 mm/s, gray). **(b)** Loading (and unloading or recovery) delays were computed with maximum cross-correlation coefficient.

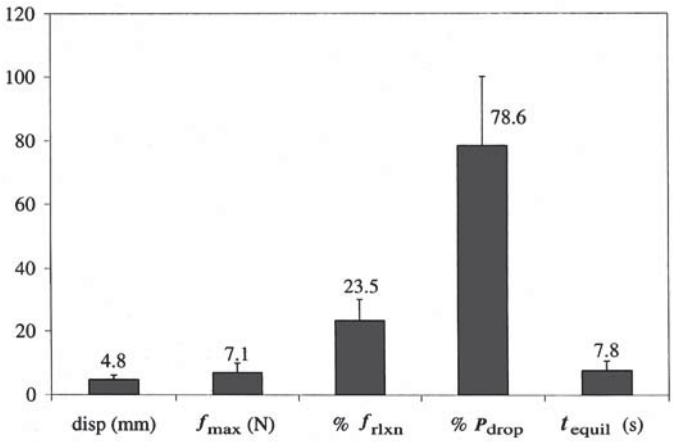

Figure 8.
Summary of mechanical (f_{max}, $\%f_{rlxn}$) and physiologic ($\%P_{drop}$, $t_{equilibrium}$) response to ramped step displacement (disp) or relaxation (rlxn) loading.

of the perfusion probe; M. DeGuia and L. Meisenheimer for their assistance with data collection and initial data processing; and S. Rhodes for her assistance with the cross-correlation study. I also thank P. Delaney and Perimed AB for their assistance with this project.

REFERENCES

1. Shurr DG, Cook TM. Prosthetics and orthotics. East Norwalk (CN): Appleton & Lange; 1990.
2. Silver-Thorn MB, Steege JW, Childress DS. A review of prosthetic interface stress investigations. J Rehabil Res Dev 1996;33(3):253–66.
3. Polliack A, Landsberger S, McNeal D, Sieh R, Craig D, Ayyappa E. Socket measurement systems perform under pressure. Biomechanics 1999;VI(6):71–80.
4. Sanders JE. Interface mechanics in external prosthetics: review of interface stress measurement techniques. Med Biol Eng Comput 1995;33:509–16.
5. Zachariah SG, Sanders JE. Interface mechanics in lower-limb external prosthetics: a review of finite element methods. IEEE Trans Rehabil Eng 1996;4(4):288–302.
6. Zhang M, Mak AFT, Roberts VC. Finite element modeling of a residual lower-limb in a prosthetic socket: A survey of development in the first decade. Med Eng Phys 1998;20:360–73.
7. Crenshaw R, Vistnes LM. A decade of pressure sore research 1977–1987. J Rehabil Res Dev 1989;26(1):63–74.
8. Daniel RK, Priest DL, Wheatley DC. Etiological factors in pressure sores: an experimental model. Arch Phys Med Rehabil 1981;62:492–98.
9. Bennett L, Lee BK. Pressure versus shear in pressure sore causation. In: Lee BK, editor. Chronic ulcers of the skin. New York: McGraw-Hill Book Co.; 1985. p. 39–56.
10. Webster JG. Prevention of pressure sores: Engineering and clinical aspects. New York: IOP Publishing, Ltd.; 1991.
11. Sanders JE, Goldstein BS, Leotta DF. Skin response to mechanical stress: adaptation rather than breakdown. J Rehabil Res Dev 1995;32(3):214–26.
12. Bader DL. The recovery characteristics of soft tissues following repeated loading. J Rehabil Res Dev 1990;27(2): 141–50.
13. Gonzalez EG, Corcoran PJ, Reyes RL. Energy expenditure in below-knee amputees: correlation with stump length. Arch Phys Med Rehabil 1974;55:111–19.
14. Waters RL, Perry J, Antonelli D, Hislop H. Energy cost of walking of amputees: the influence of level of amputation. J Bone Joint Surg Am 1976;58-A:42–46.
15. Barnes R, Thornhill B, Nix L, Rittgers S, Turley G. Prediction of amputation wound healing: roles of Doppler ultrasound and digit photoplethysmography. Arch Surg 1981;116:80–83.
16. Adera H, James K, Castronuovo J, Byrne M, Deshmukh R, Lohr J. Prediction of amputation wound healing with skin perfusion pressure. J Vasc Surg 1995;21:823–929.
17. Kram H, Appel P, Shoemaker W. Prediction of below-knee amputation wound healing using noninvasive laser Doppler velocimetry. Am J Surg 1989;158:29–31.
18. Mars M, McKune A, Robbs J. A comparison of laser Doppler fluxmetry and transcutaneous oxygen pressure measurement in the dysvascular patient requiring amputation. Eur J Vasc Endovasc Surg 1998;16:53–58.
19. Lantsberg L, Goldman M. Laser Doppler flowmetry, transcutaneous oxygen tension measurements and Doppler pressure compared in patients undergoing amputation. Eur J Vasc Surg 1991;5:195–97.
20. Ray S, Buckenham T, Belli A, Taylor R, Dormandy J. The predictive value of laser Doppler fluxmetry and transcutaneous oximetry for clinical outcome in patients undergoing revascularisation for severe leg ischemia. Eur J Vasc Endovasc Surg 1997;13:54–59.
21. Sarin S, Shami S, Shields D, Scurr J, Colerdige Smith P. Selection of amputation level: a review. Eur J Vasc Surg 1991;5:611–20.
22. Wutschert R, Bounameaux H. Determination of amputation level in ischemic limbs: reappraisal of the measurement of TCPO2. Diabetes Care 1997;20(8):1315–18.
23. Wyss C, Harrington R, Burgess E, Matsen F. Transcutaneous oxygen tension as a predictor of success after an amputation. J Bone Joint Surg 1988;70-A(2):203–7.
24. Conlon K, Sclafani L, DiResta G, Brennan M. Comparison of transcutaneous oximetry and laser Doppler flowmetry as

noninvasive predictors of wound healing after excision of extremity soft-tissue sarcomas. Surgery 1994;15(3): 335–40.

25. McMahon J, Grigg M. Predicting healing of lower limb ulcers. Aust N Z J Surg 1995;65:173–76.
26. Schubert V, Fagrell B. Local skin pressure and its effects on skin microcirculation as evaluated by laser-Doppler fluxmetry. Clin Phys 1989;9:535–45.
27. Schubert V, Fagrell B. Evaluation of the dynamic cutaneous post-ischemic hyperaemia and thermal response in elderly subjects and in an area at risk for pressure sores. Clin Phys 1991;11:169–82.
28. Salcido R, Fisher SB, Donofrio JC, Bieschke M, Knapp C, Liang R, LeGrand EK, Carney JM. An animal model and computer-controlled surface pressure delivery system for the production of pressure ulcers. J Rehabil Res Dev 1995;32(2):149–61.
29. Zhang M, Roberts C. Development of a nonlinear finite element model for analysis of stump/socket interface stresses in below-knee amputee. In: Held K, Brebbia CA, Ciskowski RD, Power H, editors. Computational biomedicine. Southhampton, UK: Computational Mechanics Publications; 1993. p. 209–14.
30. Liu GHW, Mak AFT, Lee SY. Indentation properties of the soft tissues around below-knee stumps. In: 7th World Cong. Chicago (IL): ISPO; 1992. p. 150.
31. Mak AFT, Huang L, Wang Q. A biphasic poroelastic analysis of the flow dependent subcutaneous tissue pressure and compaction due to epidermal loadings: issues in pressure sore. J Biomech Eng 1994;116:421–29.
32. Reynolds D. Shape design and interface load analysis for below-knee prosthetic sockets [dissertation]. University College London; 1988.
33. Steege JW, Schnur DS, Childress DS. Prediction of pressure at the below-knee socket interface by finite element analysis. In: Stein JL, editor. ASME Symposium on the biomechanics of normal and pathological gait; 1987; Boston, Massachusetts. New York: ASME; 1987.
34. Steege JW, Silver-Thorn MB, Childress DS. Design of prosthetic sockets using finite element analysis. In: 7th World Cong. Chicago (IL): ISPO; 1992. p. 273.
35. Torres-Moreno R. Biomechanical analysis of the interaction between the above-knee residual limb and the prosthetic socket [dissertation]. University of Strathclyde: Glasgow, Scotland, UK; 1991.
36. Vannah WM, Childress DS. Indentor tests and finite element modeling of bulk muscular tissue in vivo. J Rehabil Res Dev 1996;33(3):239–52.
37. Zhang M, Mak AFT. A finite element analysis of the load transfer between an above-knee residual limb and its prosthetic socket—roles of interface friction and distal-end boundary conditions. IEEE Trans Rehabil Eng 1996;4(4): 337–46.
38. Dinsdale SM. Decubitus ulcers: role of pressure and friction in causation. Arch Phys Med Rehabil 1974;55:147–52.
39. Husain T. An experimental study of some pressure effects on tissues, with reference to the bedsore problem. J Pathol Bact 1953;66:347–58.
40. Nola GT, Vistnes LM. Differential response of skin and muscle in the experimental production of pressure sores. Plast Reconstr Surg 1980;66(5):728–33.
41. Hall OC, Brand PW. The etiology of the neuropathic plantar ulcer. J Am Podiatr Med Assoc 1979;69(3):173–77.
42. Bennett L, Kavner D, Lee BK, Trianor FA. Shear versus pressure as causative factors in skin blood flow occlusion. Arch Phys Med Rehabil 1979;60:309–14.
43. Sangeorzan BJ, Harrington RM, Wyss CR, Czerniecki JM, Matsen FA. Circulatory and mechanical response of skin to loading. J Orthop Res 1989;7:425–31.
44. Pathak A, Silver-Thorn MB, Thierfelder CA, Prieto TE. Design of a rate-controlled indentor for in vivo analysis of residual limb tissues. IEEE Trans Rehabil Eng 1998;6(1): 12–20.
45. Silver-Thorn MB, Tonuk E. A device for viscoelastic assessment of the residual limb bulk soft tissue response to load. IEEE Eng Med Biol Mag 1999;1:646.
46. Silver-Thorn MB. In vivo indentation of lower extremity soft tissues. IEEE Trans Rehabil Eng 1999;7(3):268–77.
47. Silver-Thorn MB, Tonuk E, Kemp J. In vivo indentation of lower extremity limb soft tissues. IEEE Eng Med Biol Mag 1999;1:637.
48. Saad ZS, Ropella, KM, Cox RW, DeYoe EA. Analysis and use of fMRI response delays. Hum Brain Mapp 2001; 13:74–93.

Submitted for publication August 12, 2001. Accepted in revised form December 22, 2001.